BEAM-BEAM SIMULATION OF CRAB CAVITY WITH FREQUENCY DEPENDENT NOISE FOR LHC UPGRADE*

J. Qiang#, LBNL, Berkeley, CA94720, U.S.A.
G. Arduini, Y. Papaphilippou, T. Pieloni, CERN, Geneva, Switzerland
J. Barranco, EPFL, Lausanne, Switzerland

Abstract

High luminosity LHC upgrade will improve the luminosity of the current LHC operation by an order of magnitude [1]. Crab cavity as a critical component for compensating luminosity loss from large crossing angle collision and also providing luminosity leveling for the LHC upgrade is being actively pursued. In this paper, we will report on the study of potential effects of the frequency-dependent crab cavity noise on the beam luminosity lifetime using strong-strong beam-beam simulations.

INTRODUCTION

The crab cavity as a critical component in the LHC upgrade is being actively studied. The RF noise errors in the crab cavity could have direct impact on the colliding beams at interaction points (IPs). In a previous report [2], we studied the effects of the cavity voltage and phase white noise errors on colliding beam emittance and luminosity degradation and concluded that the rms noise amplitude level needs to be controlled within a few times10^{-5} (radian for phase and dimensionless for relative voltage amplitude error) in order to have a good luminosity lifetime. This limit might be too pessimistic since the real RF noise error inside a cavity is not a white noise but has a frequency dependency. For example, Fig. 1 shows the expected crab cavity phase noise power spectrum, based on the LHC noise spectrum, expected improvements, and feedback like bandwidth [3]. The rms amplitude in the time domain for this error is 3×10^{-4}. It is clear that this phase error is not just white noise.

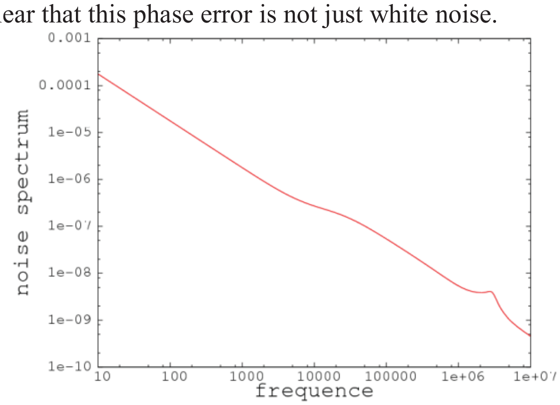

Figure 1: Power spectrum of the crab cavity RF phase noise.

*Work supported by the Director of the Office of Science of the US Department of Energy under Contract no. DEAC02-05CH11231 and by the FP7 HiLumi LHC http://hilumilhc.web.cern.ch
#jqiang@lbl.gov

COMPUTATIONAL SETUP

All simulations presented in this study were done using a strong-strong collision model implemented in the code BeamBeam3D [4]. In order to reduce numerically induced emittance growth, and to gain computational speed, the fields were computed assuming a Gaussian particle distribution, instead of a self-consistent approach.

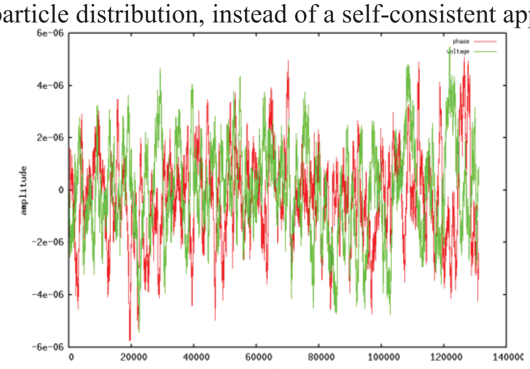

Figure 2: Phase (red) and amplitude errors of the crab cavity.

This assumption is justified by the fact that the initial Gaussian particle distribution does not change significantly in a short period of time under stable conditions. In order to keep the residual noise level low, one million macroparticles were used. The particle distribution in the longitudinal direction was divided into 8 slices. Two collisions per turn, corresponding to the interaction points (IPs) 1 and 5 in the LHC, were simulated. The crossing plane was horizontal in one IP5 (CMS experiment) and vertical in the other IP (ATLAS experiment). Linear transfer maps, calculated using the working point tunes, were employed to transfer the beam between collisions. The crab cavities are located 90 degrees phase advance from each IP. To model the beam transport through the crab cavity, we have assumed a thin lens approximation where the transfer map in the *x-z* plane is given by

$$
\begin{aligned}
x^{n+1} &= x^n \\
P_x^{\,n+1} &= P_x^{\,n} + \frac{qV}{E_s}\sin(\omega z^n / c + \phi) \\
z^{n+1} &= z^n \\
\delta E^{n+1} &= \delta E^n + \frac{qV}{E_s}\cos(\omega z^n / c + \phi) x^n \qquad (1)
\end{aligned}
$$

where V is the voltage of the crab cavity, Es is the particle energy, ϕ is the phase of the cavity, and ω is the angular frequency of the cavity. A similar transfer map with x replaced by y is used in the y-z plane. The RF noise errors in the crab cavity include both the relative voltage

ISBN 978-3-95450-147-2

amplitude error and the phase error. The phase error in the crab cavity causes beam transverse center offset at the interaction point. This is also called the zeroth order error. The RF voltage error in the crab cavity results in a tilt in the *x-z* plane or the *y-z* plane at the IPs, which can be regarded as an increase of the transverse size if projected to the *x* or *y* dimension. This is also called the first order error. In this study, we assumed that the rms phase and amplitude errors are the same. Given the noise frequency spectrum, we generated the time-dependent noise data used in the simulation. Here, we assumed that the noise errors in each crab cavity are independent of each other. In order to get the phase and voltage errors within each turn, we took 256 samplings of a white noise with a random normal distribution N(0,1) per turn to reach MHz in frequency domain, and for 131,072 turns; Then we made an FFT of the random white noise data and obtained the white noise in frequency domain. Then we multiplied that white noise data in frequency domain with the given frequency-dependent RF noise data. Here, the original frequency-dependent RF noise data was converted from dB into regular dimensionless unit. Then we made an inverse FFT of the new noise data back to the time domain. After that we selected only 1 data point for every 256 data points to obtain the turn by turn noise data used in this study. We scaled the turn-dependent noise amplitude to the nominal rms noise amplitude of 3×10^{-4}. Figure 2 shows the time evolution of the RF phase and voltage errors. There are another 14 time-dependent error data like those in Fig. 2 for 8 crab cavities used in the simulation. These noise data were read into the code during the process of simulation. The parameters used in this study are given in the following table.

Table 1: Physical Parameters Used in the Simulations

Parameter	Value
N_p [protons]	$1.1\text{-}2.2\times10^{11}$
ε_n [µm]	2.5
β^* [m]	0.15-0.60
Q_x	62.31
Q_y	60.32
Q_z	0.0019
θ [mrad]	0.59
Chromaticity	0-4
Crab cavities	on
Collisions [1/turn]	1 hor., 1 ver.

SIMULATION RESULTS

Simulation results with the frequency-dependent RF phase and voltage errors are presented here. Figure 3 shows the emittance evolution with the nominal, two times the nominal and four times the nominal noise amplitude in the simulation. Here, the nominal noise rms amplitude level is 3×10^{-4} and we have assumed 2.2×10^{11} protons bunch intensity and 0.15m beta* at the IPs. It is seen that the RF noise from the crab cavity will lead to emittance growth, and it becomes worse with larger amplitude of the noise. The initial jump of the emittance growth is due to the charge redistribution caused by the beam-beam interaction (also called dynamics beta effects) in the simulation. Figure 4 shows the luminosity evolution for these three noise amplitudes. As the noise amplitude increases, the luminosity decreases faster. In order to quantify the speed of luminosity degradation, we define a luminosity degradation rate by linearly fitting the luminosity evolution in the simulation. Figure 5 shows the luminosity degradation rate as a function of the noise amplitude with an ideal feedback model and a more

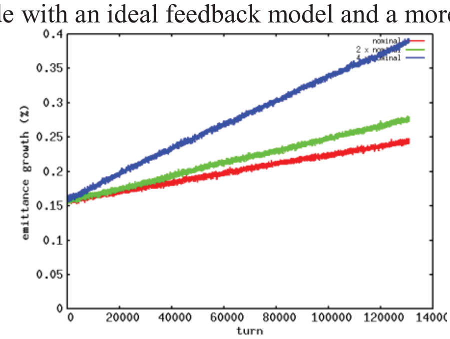

Figure 3: Emittance growth evolution with nominal, two times the nominal, and three times the nominal noise level.

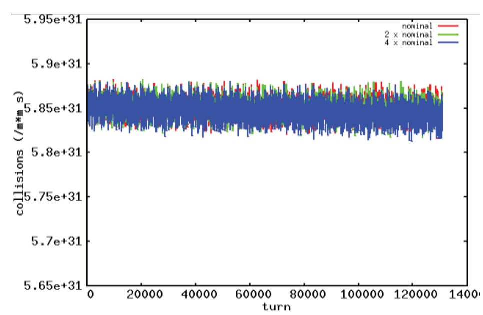

Figure 4: Luminosity evolution with nominal, two times the nominal, and three times the nominal noise level.

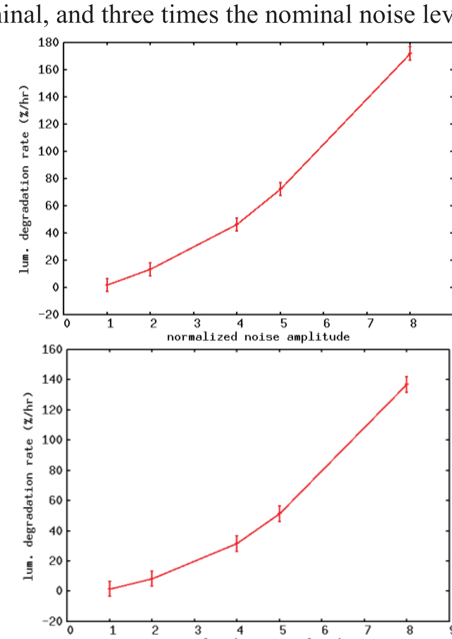

Figure 5: Luminosity degradation rate as a function of the normalized noise amplitude (here 1 corresponds to nominal 3×10^{-4} rms noise level) with a realistic feedback model (top) and with an ideal feedback model (bottom).

realistic feedback model [5]. It is seen that both models give similar results. The luminosity degradation rate grows roughly quadratic with respect to the noise amplitude. This is consistent with an analytical model proposed in [6]. In order to keep the luminosity degradation rate below 10%/hr, one should keep the noise amplitude level below one to two times the nominal amplitude level. Figure 6 shows the luminosity degradation rate as a function of the bunch intensity with the nominal noise amplitude and 0.15m beta* at the IPs. It shows relatively weaker dependence on the bunch intensity than the quadratic dependence. Figure 7 shows the luminosity degradation rate as a function of beta* at the IPs. The degradation rate falls quickly with the increase of the beta* and is roughly inversely proportional to the beta*. During the process of luminosity leveling of the HL-LHC operation, the two beams can initially collide with high intensity (2.2×10^{11}) but larger beta*. As the beam burns out, one can move to a smaller beta* to maintain a nearly flat luminosity during each run.

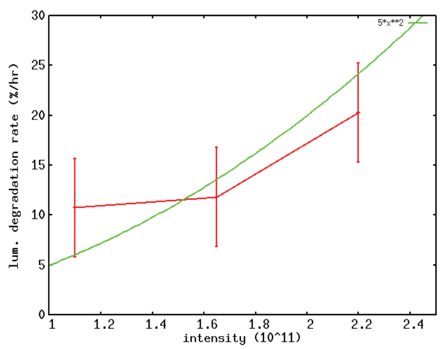

Figure 6: Luminosity degradation rate as a function of bunch intensity.

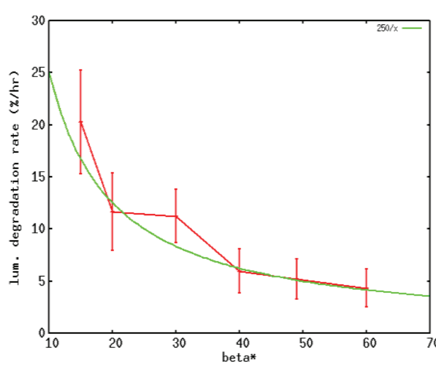

Figure 7: Luminosity degradation rate as a function of beta* at the IPs.

We also studied the sensitivity of the luminosity degradation due to the crab cavity RF errors to some machine settings such as chromaticity and tune working point. Figure 8 shows the luminosity degradation rate as a function of the machine chromaticity with 2.2×10^{11} bunch intensity, 0.15m beta* and nominal noise amplitude. It is seen that the luminosity degradation rate is quite insensitive to the variation of the machine chromaticity. Figure 9 shows the luminosity degradation rate as a function of the noise amplitude at two fraction working points (0.31,0.32) and (0.475,0.475). At both working points, the luminosity degradation rate shows similar dependence on the noise amplitude and is insensitive to the choice of these two working points.

CONCLUSIONS

In summary, we found that the tolerable rms noise amplitude with the frequency-dependent RF phase and voltage error is about a factor 10 higher than the pure white noise level obtained in our previous study. The luminosity degradation rate has a stronger dependence on the beta* at the IPs, a weaker dependence on the bunch intensity, and not very sensitive to the choice of machine chromaticity and stable working point.

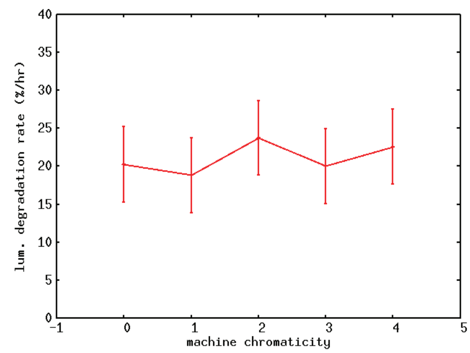

Figure 8: Luminosity degradation rate as a function of machine line chromaticity.

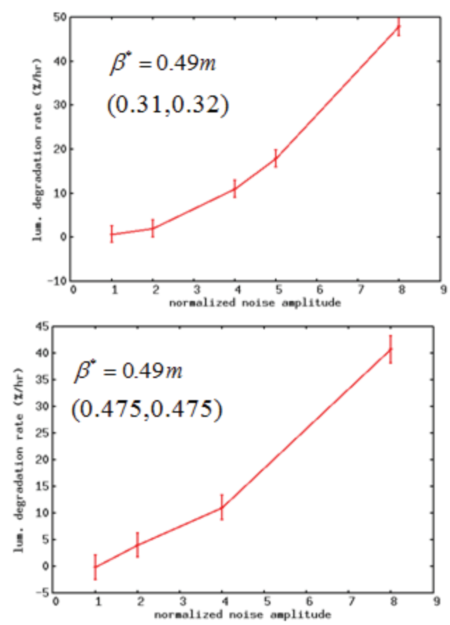

Figure 9: Luminosity degradation rate as a function of noise amplitude at machine tune working point (0.31,0.32) and working point (0.475,0.475).

ISBN 978-3-95450-147-2

REFERENCES

[1] O. S. Bruning and F. Zimmermann, in Proc. IPAC'12, New Orleans, USA, MOPPC005.
[2] J. Qiang et al., in Proc. IPAC'15, Richmond, USA, TUPTY076.
[3] T. Mastoridis and P. Baudrenghien, private communication, 2015.
[4] J. Qiang et al., J. of Comp. Phys., 198, p. 278, 2004.
[5] S. Paret and J. Qiang, in Proc. IPAC2012, New Orleans, USA, TUPPC091.
[6] K. Ohmi, in Proc. of ICFA Mini-Workshop on Beam-Beam Effects in Hadron Colliders, ed. W. Herr and G. Papotti, p. 69, 2014.